

Signal mixing in a ratchet device: commensurability and current control

Sergey Savel'ev¹, Fabio Marchesoni^{1,2}, Peter Hänggi^{1,3}, and Franco Nori^{1,4,a}

¹ Frontier Research System, The Institute of Physical and Chemical Research (RIKEN), Wako-shi, Saitama, 351-0198, Japan

² Dipartimento di Fisica, Università di Camerino, 62032 Camerino, Italy

³ Institute of Physics, University of Augsburg, Universitätsstrasse 1, 86135 Augsburg, Germany

⁴ Center for Theoretical Physics, Department of Physics, University of Michigan, Ann Arbor, MI 48109-1120, USA

Received 11 April 2004

Published online 13 July 2004 – © EDP Sciences, Società Italiana di Fisica, Springer-Verlag 2004

Abstract. Rectification current in overdamped ratchets can be easily controlled by applying two driving signals and tuning either their relative phase or their frequency ratio. The interplay of the two inputs generates intriguing transport mechanisms that can be implemented to optimize shuttling and separation of particles in a variety of physical and technological applications.

PACS. 05.40.-a Fluctuation phenomena, random processes, noise, and Brownian motion – 05.60.Cd Classical transport – 87.16.Uv Active transport processes; ion channels

1 Introduction

The net transport of particles moving out-of-equilibrium in an asymmetric substrate potential has been studied intensively for a variety of different systems [1] in order to achieve an efficient control of the net particle flow. The input signal, keeping the system out of equilibrium, can be either deterministic (i.e., ac drive) or random and time-correlated (i.e., colored noise) [2]; in particular, an ac signal can be injected so as to tilt periodically the ratchet potential (*rocked* ratchet [3]) or to modulate its amplitude with time (*pulsated* ratchet [4]). The ensuing net dc drift (the so-called ratchet current or rectification effect) occurring in these systems is important for several biological motors as well as for some technological applications; e.g., for particle separation techniques [5], smoothing of atomic surface during electromigration [6], and superconducting vortex motion control [7–13].

In this paper we study the case of a ratchet subjected simultaneously to two ac signals with periods $T_1 = 2\pi/\Omega_1$ and $T_2 = 2\pi/\Omega_2$. We focus here on the case that Ω_1/Ω_2 is rational and do not address quasi-periodic drives [14]. We consider three distinct cases: (a) the two input signals are both additive and model a doubly-rocked ratchet; (b) both signals are coupled multiplicatively to the ratchet potential thus resulting in a doubly pulsated ratchet; (c) one signal ac drives the ratchet, while the other one multiplicatively modulates its amplitude (rocked-pulsated ratchet).

A variety of tunable physical systems can be effectively controlled through the combined action of two (either independent or correlated) applied signals, like asymmetric SQUIDS [15,16] and Josephson junctions arrays [17], colloids in arrays of optical tweezers [18], interacting binary mixtures driven on (asymmetric) periodic substrates [19], ferrofluids [20], dislocation transport in crystalline solids [21,22], electron pumping in quantum dots [23].

The key result of this paper (see also [24]) is that, no matter how we feed two periodic signals into a ratchet device, *signal mixing* determines a rich behavior of the ratchet dynamics depending on the input signal parameters (frequency, amplitude and phase). In particular, we prove that *rectification* of a primary signal by a ratchet *can be controlled more effectively by applying a secondary (additive or multiplicative) signal with tunable frequency and phase*, than by tinkering with the ratchet potential – mostly modelling an uncontrollable substrate. As in the overdamped, adiabatic regime the complication of chaos is absent, tuning the relative phase and the frequency ratio of the mixing drives provides a convenient and versatile way of inducing particle transport in a ratchet.

2 Model

Let us consider the simplest possible deterministic ratchet model: an overdamped Brownian particle $x(t)$ diffusing in a piecewise linear asymmetric potential $V_0(x)$ (shown in

^a e-mail: nori@umich.edu

Fig. 1a). Two rectangular input signals,

$$A_i(t) = A_i \operatorname{sgn}[\cos(\Omega_i t + \phi_i)] \quad (1)$$

with $i = 1, 2$, $A_i \geq 0$, and $\operatorname{sgn}[\dots]$ denoting the sign of its argument [...], act on the particle according to the Langevin equation

$$\dot{x} = -V'(x, t) + A_a(t) + \xi(t), \quad (2)$$

where $\xi(t)$ is a stationary Gaussian white noise with $\langle \xi(t) \rangle = 0$ and $\langle \xi(t)\xi(0) \rangle = 2D\delta(t)$, and

$$V(x, t) = V_0(x)[1 + A_m(t)]. \quad (3)$$

Note that the noise strength D is proportional to the temperature, i.e., $D \propto T$. Equation (1) allows two distinct ways of coupling an additional control signal $A_2(t)$ to a rocked ratchet driven by $A_1(t)$:

(a) doubly-rocked ratchet:

$$A_m(t) = 0, \quad A_a(t) = A_1(t) + A_2(t); \quad (4)$$

(b) doubly-pulsated ratchet

$$A_a(t) = 0, \quad A_m(t) = A_1(t) + A_2(t) \quad (5)$$

with $A_1 + A_2 \leq 1$

(c) rocked-pulsated ratchet:

$$A_a(t) = A_1(t), \quad A_m(t) = A_2(t) \quad (6)$$

with $A_2 \leq 1$.

In our analytical discussion we assume that Brownian relaxation takes place on a much shorter time scale than either both periods T_1 and T_2 (fully adiabatic), or one period, T_1 or T_2 (partially adiabatic). We also present results for the fully non-adiabatical case when both periods are comparable with relaxation time. Without loss of generality, adopting a piecewise linear substrate potential $V_0(x)$, like in Figure 1a, greatly simplifies our presentation.

Our results are obtain by using three different approaches.

- Direct simulation of the Langevin equation (2).
- Fully adiabatic calculations based on the Fokker-Planck equation for the probability density $P(x, t)$ (see, e.g., [1]):

$$\frac{\partial P}{\partial t} = \frac{\partial}{\partial x} \left\{ (V_0' [1 + A_m] - A_a) P + D \frac{\partial P}{\partial x} \right\}. \quad (7)$$

This equation can be rewritten in a fully adiabatic approximation as

$$j_{\text{inst}}(A_a(t), A_m(t)) = (V_0' [1 + A_m] - A_a) P + D \frac{\partial P}{\partial x}, \quad (8)$$

where the current $j_{\text{inst}}(t)$ corresponds to the Stratonovich solution and depends on the instantaneous values of A_a and A_m (see, e.g., [1]). The average over the smallest common period \tilde{T} for both applied signals is obtained by numerical integration:

$$j = \frac{1}{\tilde{T}} \int_0^{\tilde{T}} j_{\text{dc}}(A_a(t), A_m(t)) dt. \quad (9)$$

- Analytical calculations developed for several special cases.

3 Doubly-rocked ratchet

3.1 Fully adiabatic limit

The advantage of taking the *fully adiabatic* limit ($\Omega_1, \Omega_2 \rightarrow 0$) is that the output $j(\Omega_1, \Omega_2, A_1, A_2)$ of a doubly rocked ratchet is expressible analytically in terms of the current $j_R(A)$ of the well-studied one-frequency rocked ratchet [3], corresponding to setting $A_1 = A$, $A_2 = 0$ with $\Omega_1 \rightarrow 0$ (Fig. 1b). Note that here $j_R(A)$ is a symmetric function of A , $j_R(A) = A[\mu(A) - \mu(-A)]/2$, where $\mu(A)$ is the mobility of an overdamped particle running down the tilted ratchet potential $V_0(x) - Ax$. By inspecting Figure 1c, one concludes that the overall ratchet current $j(\Omega_1, \Omega_2, A_1, A_2)$ results from the interplay of the two usual one-frequency currents, $j_R(A_1 + A_2)$ and $j_R(A_1 - A_2)$, driven by the ac amplitudes $A_1 + A_2$ and $A_1 - A_2$, respectively. That is

$$j(\Omega_1, \Omega_2 = \Omega_1 \frac{2m-1}{2n-1}, A_1, A_2) = j_{\text{avg}}(A_1, A_2) - \frac{(-1)^{m+n} p(\Delta_{n,m})}{(2m-1)(2n-1)} \Delta j(A_1, A_2),$$

$$j(\Omega_1, \Omega_2 \neq \Omega_1 \frac{2m-1}{2n-1}, A_1, A_2) = j_{\text{avg}}(A_1, A_2), \quad (10)$$

with $\Delta_{n,m} = (2n-1)\phi_2 - (2m-1)\phi_1, \operatorname{mod}(2\pi)$,

$$j_{\text{avg}}(A_1, A_2) = \frac{1}{2} [j_R(A_1 - A_2) + j_R(A_1 + A_2)], \quad (11)$$

$$\Delta j(A_1, A_2) = \frac{1}{2} [j_R(A_1 - A_2) - j_R(A_1 + A_2)], \quad (12)$$

for any integers m, n and $m > n$. The ϕ_1, ϕ_2 modulation is fully described by the multiplicative phase factor

$$p(\phi) = \frac{|\pi - \phi|}{\pi} - 0.5. \quad (13)$$

We make now a few relevant remarks;

1. The doubly rocked ratchet current (in the fully adiabatic limit) is insensitive to Ω_1, Ω_2 , unless $\Omega_2/\Omega_1 = (2m-1)/(2n-1)$. Its intensity coincides with the “baseline” value $j_{\text{avg}}(A_1, A_2)$ of equation (11); spikes with decreasing amplitude $\Delta j(A_1, A_2)/(2m-1)(2n-1)$ show up at the higher odd fractional harmonics;
2. The sign of the spike factor $\Delta j(A_1, A_2)$ is sensitive to the signal amplitudes A_1, A_2 . For instance, if we choose A_1, A_2 so that $A_1 + A_2$ and $|A_1 - A_2|$ fall onto the rising (decaying) branch of $j(A)$ in Figure 1b, then $\Delta j(A_1, A_2)$ is negative (positive) (see, Figs. 2a and b);
3. The current spikes at $\Omega_2/\Omega_1 = (2m-1)/(2n-1)$ depend on the initial value of ϕ_2 , and for a fixed ϕ_1 , their amplitude oscillates proportional to the modulation factor $p(\Delta_{n,m})$ (see, Figs. 2a and c).

All these properties are illustrated in Figure 2, where results from numerical simulation are displayed. We remark that the overall sign of our doubly rocked ratchet is always determined by the polarity of $V_0(x)$ (positive in Fig. 1a), as $|\Delta j(A_1, A_2)| < |j_{\text{avg}}(A_1, A_2)|$ for any choice of A_1, A_2 .

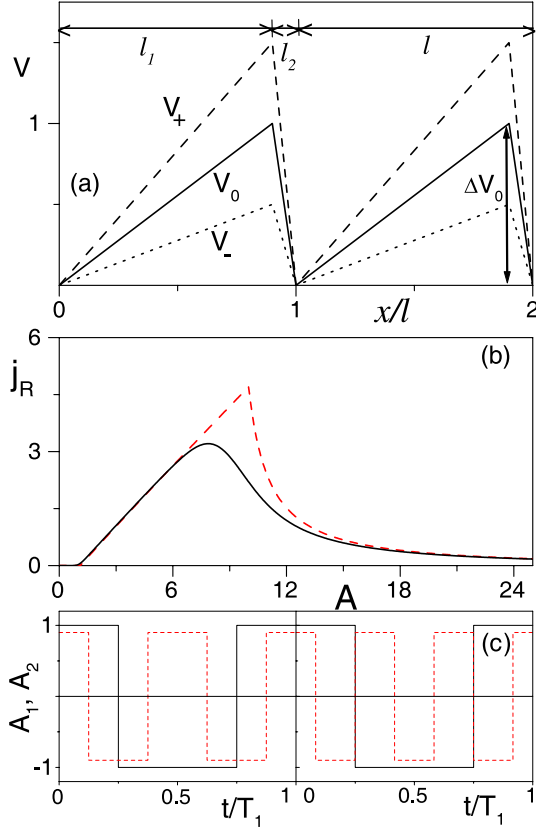


Fig. 1. (a) Ratchet potentials. High V_+ and low V_- barrier configurations of the modulated potential $V(x, t)$, i.e. $V_{\pm}(x) = V_0(x)(1 \pm A_2)$ (dashed V_+ and dotted V_- curves) with $A_2 = 0.5$. Reference ratchet potential (solid curve): $V_0(x) = qx/l_1$ for $0 < x < l_1$; $= q - q(x - l_1)/l_2$ for $l_1 < x < l = l_1 + l_2$, with $q = 1$, $l_1 = 0.9$, and $l = 1$; the barrier height ΔV_0 coincides with q . (b) Response curve $j_R(A)$ of the potential $V_0(x)$ driven by a rectangular force $A_1(t)$ with $A_1 = A$ ($A_2 = 0$) in the adiabatic limit $\Omega_1 \rightarrow 0$ at zero temperature $D = 0$ (dashed curve), and low temperature $D/\Delta V_0 = 0.05$ (solid curve). (c) Input signals $A_1(t)$ (solid), and $A_2(t)$ (dashed) with $\Omega_2 = 3\Omega_1$ (right panel) and $\Omega_2 = 2\Omega_1$ (left panel); also: $\phi_1 = \phi_2 = 0$, $A_1 = 1$, and $A_2 = 0.9$.

3.2 Partially adiabatic limit

In the *partially adiabatic* regime, where only one frequency tends to zero (say, $\Omega_1 \rightarrow 0$) multiple current inversions are possible (Fig. 3). The underlying mechanism hinges on the step structure of the one-frequency rocked ratchet current of particles, travelling in a tilted potential $V_0 \mp |A_1|x$, for the non-adiabatic regime, where Ω_2 is small but finite [3]. For instance, in the limit $\Omega_1 \rightarrow 0$ the net current of the doubly-rocked ratchet (a) can be easily approximated to

$$j(\Omega_1 \ll \Omega_2, A_1, A_2) = \frac{1}{2}[j_+(\Omega_2, A_2) + j_-(\Omega_2, A_2)], \quad (14)$$

where $j_{\pm}(\Omega_2, A_2)$ is the average current across the static tilted ratchet potential $V_0(x) \mp |A_1|x$ driven by the rectangular signal $A_2(t)$. Note that for $\Omega_2 \gg \Omega_1$ the commensuration spikes (10) can be neglected as they decay proportional to Ω_1/Ω_2 .

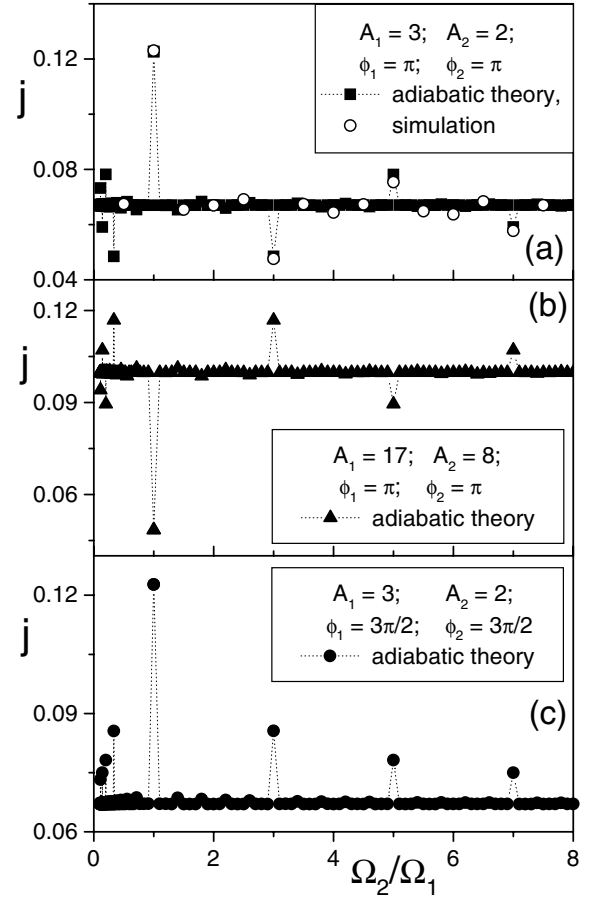


Fig. 2. Rectified current in a doubly-rocked ratchet with $V_0(x)$ as in Figure 1a and driven by two rectangular signals $A_1(t)$, $A_2(t)$ and temperature or noise $D = 0.6$. (a) Numerical simulations for $\phi_1 = \phi_2 = \pi$ and $\Omega_1 = 0.01$ (open circles) and fully adiabatic approximation (solid squares). The amplitudes of the driving forces are chosen in a rising interval of the one-frequency rocked ratchet current j_R , namely, $A_1 = 3$ and $A_2 = 2$. (b) The same as in (a) but for amplitudes $A_1 = 17$ and $A_2 = 8$ which correspond to the decreasing amplitude interval of j_R . Ω_1 was kept constant and Ω_2 increased. In agreement with the derived equations (10–12), the spikes of the currents in (a) and (b) are inverted. (c) The same as in (a) but for different phases of driving signals: $\phi_1 = \phi_2 = 3\pi/2$. Spikes in (a) and (c) evolve in agreement with the modulation factor $p(\Delta_{n,m})$

In order to clarify the resulting current structure (14), in Figure 3 we consider the simplified case $A_1 = A_2 \equiv A$ and $\Omega_2 \gg \Omega_1$. During one half of the longer period $T_1/2$, the total ac force $A_a(t)$ switches many times either between 0 and $2A$, or between 0 and $-2A$ with frequency Ω_2 . We also assume that the higher forcing frequency Ω_2 is lower than the deterministic relaxation rate $\Omega_q = \pi q/l_1^2$, i.e., the Brownian particle reaches a $V_0(x)$ minimum during each half period $T_2/2$ when $A_a(t) = 0$. As a consequence, the particle moves an integer number of unit cells l during each short period T_2 . A straightforward analytical calculation of the average particle velocity to the right

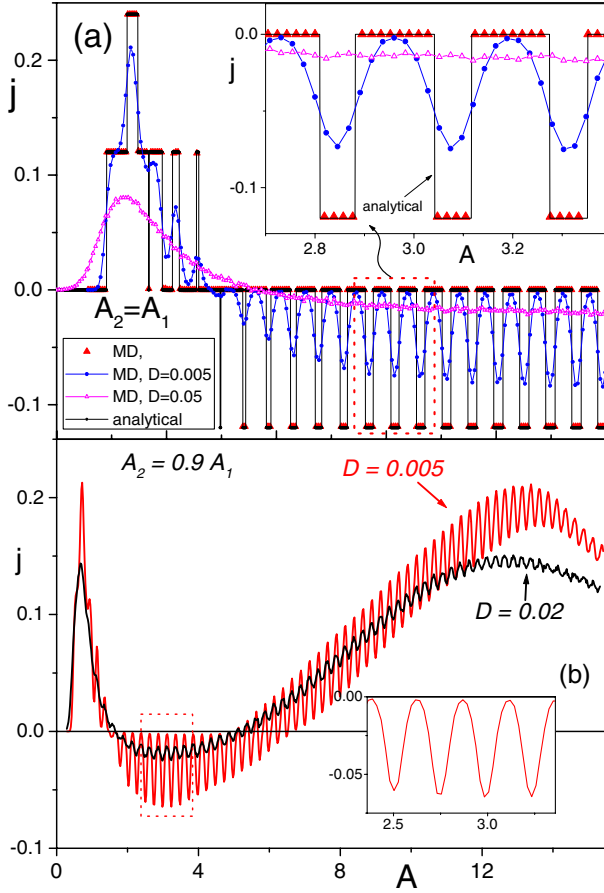


Fig. 3. Rectified current in the doubly-rocked ratchet with $T_1 = 10^3$, $T_1/T_2 = 240$. Potential parameters are $q = 0.4$, $l_1 = 0.7$, and $l = 1$. (a) Simulation data for $A_1 = A_2 = A$, $D = 0$ (red solid triangles), 5×10^{-3} (blue dots), 0.05 (pink open triangles). The black solid curve with steps is our analytical prediction for $D = 0$ (see text). Inset in (a): blow-up of all curves in the dashed window of (a). (b) Simulation data for $A_2 = 0.9A_1$, $A_1 = A$, $D = 0.005$ (thin (red) curve) and $D = 0.02$ (thick (black) curve). Inset in (b): blow-up of the thin curve ($D = 0.005$).

(left) yields

$$v_{\pm}(A) = \pm nl/T_2 \quad \text{for} \quad A_{\pm}^{(n+1)} < A < A_{\pm}^{(n)} \quad (15)$$

and

$$v_{\pm}(A) = 0, \quad \text{for} \quad A < A_{\pm}^{(1)}, \quad (16)$$

with

$$A_{\pm}^{(n)} = \frac{1}{2} \left\{ \frac{(2n-1)l \pm \delta l}{2T_2} \mp f_{\text{differ}} + \sqrt{\left[\frac{(2n-1)l \pm \delta l}{2T_2} \pm f_{\text{differ}} \right]^2 + \frac{Q^2}{l_1 l_2} + \frac{2Q}{T_2}} \right\}, \quad (17)$$

$f_{\text{differ}} = Q\delta l/(2l_1 l_2)$, and $\delta l = l_1 - l_2$. The analytical expression $j = (v_+(A) + v_-(A))/2$ for the ratchet current

compares very well with the simulation data displayed in Figure 3a. We notice that on increasing A the resulting ratchet current develops a negative tail made of entrained rectangular teeth of the same size. Such a negative tail persists in the presence of noise, although the teeth get gradually suppressed, thus implying, at variance with the fully adiabatic limit, a robust inverted output signal.

Finally, for $A_2/A_1 < 1$ the particle current j depends on the driving amplitude in a much more complicated manner, though still expressible in terms of equation (14). For a small relative difference of ac amplitudes, $A_1 - A_2 \ll A_1$, the current $j(A)$ exhibits multiple current inversions, as seen in Figure 3b. Noise smooths out the sharp peaks in $j(A)$ (Figs. 3a and b).

4 Doubly-pulsated ratchet

Here the Brownian particle diffuses in a pulsated potential $V(x, t)$, whose amplitude switches among four different values $\Delta V_0(1 - A_1 - A_2)$, $\Delta V_0(1 + A_1 - A_2)$, $\Delta V_0(1 - A_1 + A_2)$, and $\Delta V_0(1 + A_1 + A_2)$. As $m > n$, let us consider the two time-dependent potentials $V_0(x)[1 - A_1 + A_2(t)]$, for the half cycle $A_1(t) = -A_1$, and $V_0(x)[1 + A_1 + A_2(t)]$, for the remaining half cycle $A_1(t) = A_1$: They are both pulsated at the higher frequency Ω_2 and, therefore, sustain positive currents, $j_{p1}(A_2)$ and $j_{p2}(A_2)$, respectively (proportional to Ω_2^2 for $\Omega_1 \rightarrow 0$, e.g., [1]). Following the approach outlined in the previous case (a), and guided by the plots of $A_1(t)$, $A_2(t)$ in Figure 1c, one concludes that equation (10) applies to the present case, too, after replacing definition (11) with

$$j_{\text{avg}}(A_1, A_2) = \frac{1}{2} [j_{p1}(A_2) + j_{p2}(A_2)]. \quad (18)$$

Note that here the sign of j_{avg} is reversed with respect to case (a). For $\Omega_2 = (2m - 1)\Omega_1$ one recognizes immediately the existence of an odd harmonics structure in the spectrum of the ratchet current, but, at variance with equation (10), no obvious factorization between the A_1 , A_2 dependence and m , ϕ_2 modulation could be derived, as the adiabatic approximation is no longer tenable here. Nevertheless, even in this case, the spike amplitudes are still inversely proportional to the ratio Ω_2/Ω_1 . Numerical simulations in Figure 4 support these predictions.

5 Rocked-pulsated ratchet

The mixing of an additive and a multiplicative signal provides a *control mechanism* of potential interest in device design. In the *fully adiabatic* limit, the ac driven Brownian particle can be depicted as moving back and forth over two alternating ratchet potentials

$$V_{\pm}(x) = V_0(x)(1 \pm A_2). \quad (19)$$

Both potential configurations $V_{\pm}(x)$ are capable of rectifying the additive driving signal $A_1(t)$; the relevant net

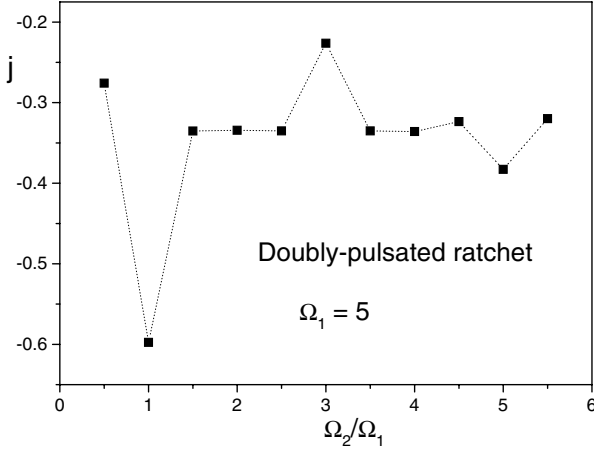


Fig. 4. Rectified current in the doubly pulsated ratchet of Figure 1a driven by two square-wave signals $A_1(t)$, $A_2(t)$ with $\phi_1 = \phi_2 = \pi$ and $A_1 = A_2 = 0.5$ (molecular dynamics simulation). Other parameter values: $q = 2$, $l_1 = 0.9$, $l = 1$ and $D = 0.6$.

currents $\bar{j}_{\pm}(A_1)$ are related to the curve $j_R(A)$ plotted in Figure 1b:

$$\bar{j}_{\pm}(A_1) = (1 \pm A_2) j_R \left[\frac{A_1}{1 \pm A_2} \right],$$

with $D \rightarrow D/(1 \pm A_2)$. (20)

On separating the time interval $(2n-1)T_1$ into an uncorrelated sequence of $(2m-1)$ shorter driving cycles T_2 along $V_{\pm}(x)$ (we assumed $m > n$, see Fig. 1c), one eventually casts the total ratchet current in the form (10) with

$$j_{\text{avg}}(A_1, A_2) = (1/2)[\bar{j}_-(A_1) + \bar{j}_+(A_1)], \quad (21)$$

$$\Delta j(A_1, A_2) = (1/2)[\bar{v}_-(A_1) - \bar{v}_+(A_1)], \quad (22)$$

where

$$\bar{v}_{\pm}(A_1) = A_1[\mu_{\pm}(A_1) + \mu_{\pm}(-A_1)]/2. \quad (23)$$

We recall that in our notation $\mu_{\pm}(A)$ is the static mobility of the tilted potentials $V_{\pm}(x) - Ax$.

It is easy to check that $|\Delta j(A_1, A_2)|$ may grow larger than $|j_{\text{avg}}(A_1, A_2)|$ and, therefore, current reversal may take place for appropriate values of the model parameters, as shown by the simulation results of Figure 5a. In fact, a relatively small modulation of the ratchet potential amplitude at low temperatures can easily reverse the polarity of the simply rocked ratchet $V_0(x)$. Let us consider the simplest case possible, $\Omega_1 = \Omega_2$ and $\phi_1 = \phi_2$: As the ac drive points in the “easy” direction of $V_0(x)$, namely to the right, the barrier height $V(x, t)$ is set at its maximum value $\Delta V_0(1 + A_2)$; at low temperatures the Brownian particle cannot overcome it within a half ac-drive period $T_1/2$. In the subsequent half period the driving signal $A_1(t)$ changes sign, thus pointing against the steeper side of the $V(x, t)$ wells, while the barrier height drops to its minimum value $\Delta V_0(1 - A_2)$: Depending on the value of $\Delta V_0/D$, the particle may have a better chance

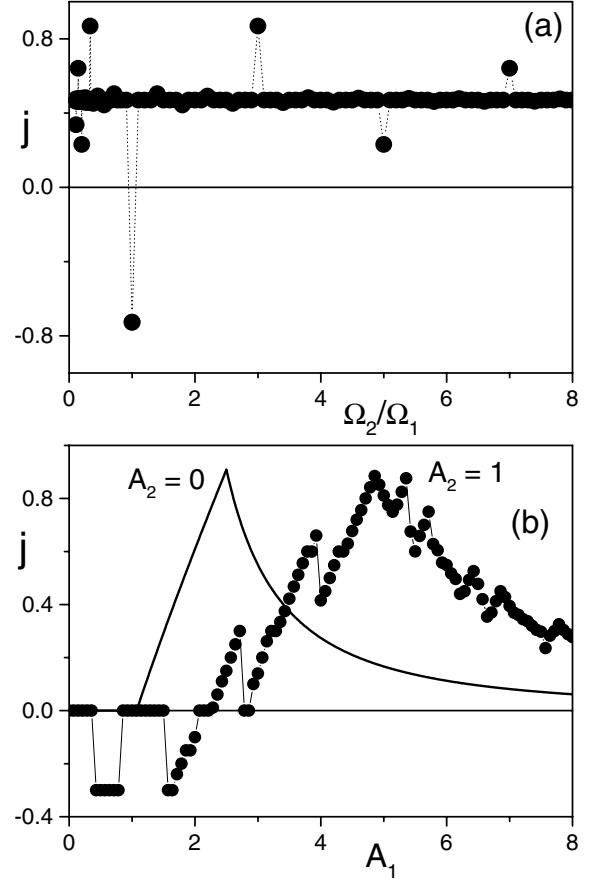


Fig. 5. (a) Rectified current in a rocked-pulsated ratchet in the fully adiabatic regime. Additive signal $A_1(t)$, with $A_1 = 4$ and $\Omega_1 = 0.01$, and modulating signal $A_2(t)$, with $A_2 = 0.5$; both signals are in-phase: $\phi_1 = \phi_2 = \pi$; noise level: $D = 0.4$. $V_0(x)$ parameters are: $q = 2$, $l_1 = 0.9$, $l = 1$. (b) Rectified current in a rocked-pulsated ratchet in the partially adiabatic regime. Drive parameters: $T_1 = 10^3$, $T_1/T_2 = 600$, $\phi_1 = \phi_2 = 0$, $A_2 = 1$ (black dots) and 0 (solid curve); $D = 0$. $V_0(x)$ parameters are: $q = 0.75$, $l_1 = 0.7$, $l = 1$.

to escape a potential well to the left than to the right, thus making a current reversal possible. Of course, the net current may be controlled via the modulation parameters A_2 and ϕ_2 , too.

For both the doubly-rocked and rocked-pulsated ratchets, equation (10) is symmetric under $m \leftrightarrow n$ exchange; this implies that, as long as the fully adiabatic approximation is tenable, each spectral spike (m, n) of the ratchet current is mirrored by a spike (n, m) of equal strength (see Figs. 2 and 5). This is not true, e.g., in the *partially adiabatic* regime, where the dynamics depends critically on whether Ω_1/Ω_2 or Ω_2/Ω_1 tends to zero.

In the partly adiabatic limit $\Omega_2 \ll \Omega_1$, additional current inversions are observed for the rocked-pulsated ratchet (Fig. 5b). In order to understand the mechanism of the negative-current rectangular-shape peaks for small driving amplitudes A , let us consider the simplest possible case when $A_2 = 1$, i.e., the potential $V(x, t)$ is switched off completely during the “idle” half of the shorter period

(i.e., when $A_2(t) = -A_2$). Thus, a particle, captured in a potential minimum when $V(x, t)$ is switched on, starts freely moving to the right if $A_1(t) = A_1$ or to the left if $A_1(t) = -A_1$ when $V(x, t) = 0$. In order to move to the neighboring potential cell, the particle has to travel further than the location of a potential maximum $V_0(x)$ during the “idle” time. Since the left maximum is the closest one, the particle moves on average to the left for low amplitudes. The interval of amplitudes, $A_{\text{run}} < A < A_{\text{stop}}$ corresponding to the first negative peak can be easily calculated by imposing the condition that the particle has enough time to reach the location of the left potential maximum during $T_2/2$ but cannot reach the right one spending the same amount of time, i.e., $A_{\text{run}} \cdot (T_2/2) = l_2$ and $A_{\text{stop}} \cdot (T_2/2) = l_1$. These equations provide the values $A_{\text{run}} = 0.36$ and $A_{\text{stop}} = 0.84$. These values perfectly agree with our simulations (see, Fig. 5b). At higher values of A_1 the asymmetry of the potential during the “active” half of the shorter period (i.e., when the potential is switched on: $A_2(t) = A_2$) is responsible for the rectification. Thus, the current becomes positive in agreement with the polarity of the potential V_+ .

6 Conclusions

We have presented an intriguing signal mixing approach that can be implemented to obtain directed transport on the mesoscopic and nano-scales. It might be used to optimize transport in colloidal systems, vortex matter and other soft-matter systems.

The effects discussed here should not be mistaken for a manifestation of harmonic mixing (HM) [25–31], namely the mechanism where two or more linearly superimposed periodic input signals may develop a phase dependent dc output as an effect of nonlinearity. Transport in a binary mixture [32] allows to discriminate between nonlinearity induced signal mixing (like HM) and asymmetry induced signal mixing (like in the cases discussed here). Namely, nonlinearity and asymmetry may result in current spikes corresponding to different winding numbers of the two mixing frequencies [32].

The stay of F.M. at RIKEN was supported by a Canon Foundation Europe award. We acknowledge support from the US NSF grant No. EIA-0130383 (F.N.) and the Deutsche Forschungsgemeinschaft via SFB-486 (P.H.).

References

1. P. Reimann, Phys. Rep. **361**, 57 (2002); R.D. Astumian, Science **276**, 917 (1997); F. Jülicher, A. Ajdari, J. Prost, Rev. Mod. Phys. **69**, 1269 (1997); R.D. Astumian, P. Hänggi, Physics Today **55**(11), 33 (2002); H. Linke, Appl. Phys. A **75**, 167 (2002), special issue on Brownian motors
2. C.R. Doering, W. Horsthemke, J. Riordan, Phys. Rev. Lett. **72**, 2984 (1994); R. Bartussek, P. Reimann, P. Hänggi, Phys. Rev. Lett. **76**, 1166 (1996)
3. R. Bartussek, P. Hänggi, J.P. Kissner, Europhys. Lett. **28**, 459 (1994)
4. R.D. Astumian, M. Bier, Phys. Rev. Lett. **72**, 1766 (1994)
5. J. Rousselet, L. Salome, A. Ajdari, J. Prost, Nature **370**, 446 (1994)
6. I. Derényi, C. Lee, A.L. Barabási, Phys. Rev. Lett. **80**, 1473 (1998)
7. J.F. Wambaugh, C. Reichhardt, C.J. Olson, F. Marchesoni, F. Nori, Phys. Rev. Lett. **83**, 5106 (1999)
8. C.J. Olson, C. Reichhardt, B. Jankó, F. Nori, Phys. Rev. Lett. **87**, 177002 (2001)
9. F. Marchesoni, B.Y. Zhu, F. Nori, Physica A **325**, 78 (2003)
10. B.Y. Zhu, F. Marchesoni, F. Nori, Physica E **18**, 318 (2003); B.Y. Zhu, F. Marchesoni, F. Nori, Phys. Rev. Lett. **92**, 180602 (2004)
11. B.Y. Zhu, F. Marchesoni, V.V. Moshchalkov, F. Nori, Phys. Rev. B **68**, 014514 (2003); B.Y. Zhu, F. Marchesoni, V.V. Moshchalkov, F. Nori, Physica C **388**, 665 (2003); B.Y. Zhu, F. Marchesoni, V.V. Moshchalkov, F. Nori, Physica C **404**, 260 (2004)
12. J.E. Villegas, S. Savel'ev, F. Nori, E.M. Gonzalez, J.V. Anguita, R. García, J.L. Vicent, Science **302**, 1188 (2003)
13. S. Savel'ev, F. Nori, Nature Materials **1**, 179 (2002)
14. E. Neumann, A. Pikovsky, Eur. Phys. J. B **26**, 219 (2002)
15. I. Zapata, R. Bartussek, F. Sols, P. Hänggi, Phys. Rev. Lett. **77**, 2292 (1996); I. Zapata, J. Luczka, F. Sols, P. Hänggi, Phys. Rev. Lett. **80**, 829 (1998)
16. A. Sterck, S. Weiss, D. Koelle, Appl. Phys. A **75**, 253 (2002); S. Weiss, D. Koelle, J. Müller, R. Gross, K. Barthel, Europhys. Lett. **51**, 499 (2000)
17. F. Falo, P.J. Martínez, J.J. Mazo, S. Cilla, Europhys. Lett. **45**, 700 (1999); J.B. Majer, J. Peguiron, M. Grifoni, M. Tusveld, J.E. Mooij, Phys. Rev. Lett. **90**, 056802 (2003)
18. P.T. Korda, M.B. Taylor, D.G. Grier, Phys. Rev. Lett. **89**, 128301 (2002)
19. S. Savel'ev, F. Marchesoni, F. Nori, Phys. Rev. Lett. **91**, 010601 (2003)
20. A. Engel, H.W. Müller, P. Reimann, A. Jung, Phys. Rev. Lett. **91**, 060602 (2003)
21. F. Marchesoni, Phys. Rev. Lett. **77**, 2364 (1996); G. Costantini, F. Marchesoni, Phys. Rev. Lett. **87**, 114102 (2001)
22. A.L. Sukstanskii, K.I. Primak, Phys. Rev. Lett. **75**, 3029 (1995); M. Salerno, Y. Zolotaryuk, Phys. Rev. E **65**, 056603 (2002)
23. M. Switkes, C.M. Marcus, K. Campman, A.C. Gossard, Science **283**, 1905 (1999)
24. S. Savel'ev, F. Marchesoni, P. Hänggi, F. Nori, Europhys. Lett. **67**, 179 (2004)
25. F. Marchesoni, Phys. Lett. A **119**, 221 (1986)
26. W. Wonneberger, Solid State Commun. **30**, 511 (1979)
27. I. Goychuk, P. Hänggi, Europhys. Lett. **43**, 503 (1998)
28. J. Lehmann, S. Kohler, P. Hänggi, A. Nitzan, J. Chem. Phys. **118**, 3283 (2003)
29. J. Luczka, R. Bartussek, P. Hänggi, Europhys. Lett. **31**, 431 (1995); P. Hänggi, R. Bartussek, P. Talkner, J. Luczka, Europhys. Lett. **35**, 315 (1996)
30. R. Guantes, S. Miret-Artés, Phys. Rev. E **67**, 046212 (2003)
31. M. Barbi, M. Salerno, Phys. Rev. E **63**, 066212 (2001)
32. S. Savel'ev, F. Marchesoni, F. Nori, Phys. Rev. Lett. **92**, 160602 (2004)